IEEE Photonics Journal
An IEEE Photonics Society Publication

Open Access

Breather and Pulse-Package Dynamics in Multinonlinear Electrooptical Systems With Delayed Feedback

Volume 8, Number 4, August 2016

Alain F. Talla
Romain Martinenghi
Paul Woafo
Yanne K. Chembo, Senior Member, IEEE

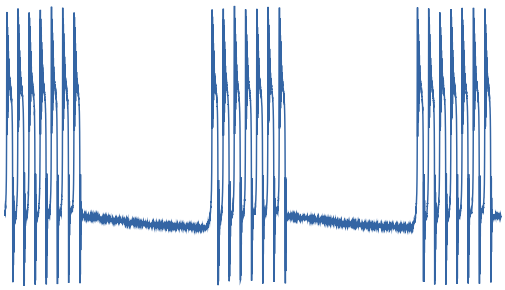

DOI: 10.1109/JPHOT.2016.2593790
1943-0655

IEEE photonics SOCIETY

IEEE

Breather and Pulse-Package Dynamics in Multinonlinear Electrooptical Systems With Delayed Feedback

Alain F. Talla,[1] Romain Martinenghi,[2] Paul Woafo,[1,3] and Yanne K. Chembo,[2] *Senior Member, IEEE*

[1]Laboratory of Modelling and Simulation in Engineering, Biomimetics and Prototypes, Department of Physics, Faculty of Science, University of Yaoundé, Yaoundé, Cameroon
[2]Department of Optics, FEMTO-ST Institute (CNRS UMR6174), Université Bourgogne-Franche-Comté, 25030 Besançon cedex, France
[3]Applied Physics Research Group (APHY), Vrije Universiteit Brussel, 1050 Brussels, Belgium

DOI: 10.1109/JPHOT.2016.2593790

Manuscript received June 27, 2016; accepted July 19, 2016. Date of current version August 3, 2016. The work of Y. K. Chembo was supported by the European Research Council project Next-Phase, by the Centre National d'Études Spatiales project SHYRO, by the project CORPS (*Région de Franche-Comté*), and by the Laboratoire d'Excellence ACTION. Corresponding author: Y. K. Chembo (e-mail: yanne.chembo@femto-st.fr).

Abstract: We investigate the temporal dynamics of a multinonlinear electrooptical system with delayed feedback. We show that when a self-sustained electronic oscillator is introduced in the electric path of the feedback loop, a wide variety of complex periodic and chaotic states can be excited. In particular, the chaotic breather and pulse-package oscillations with slow–fast temporal dynamics are experimentally observed in the system, and they are characterized by excitablelike trajectories and scroll patterns in the state space. We show that a notable specificity of these chaotic states is the presence of three distinct and well-separated timescales in the temporal time traces. We analyze the interaction between the main nonlinearities of the system and the delayed feedback loop, and finally, we discuss the main dynamical features displayed by this family of photonic systems.

Index Terms: Nonlinear oscillations, breather dynamics, electrooptical system, delayed feedback, chaos.

1. Introduction

Photonic systems with delayed feedback have been the focus of intense research activities in recent years. These systems have been shown to be excellent platforms to investigate the interaction between the complexity induced by nonlinearity and the infinite dimensionality inherent to the time-delay [1]–[4].

In this regard, electro-optical (or optoelectronic) oscillators with delayed feedback have been investigated extensively from both the fundamental and applied points of view. These systems have been originally introduced by Neyer and Voges in [5] as an integrated optics implementation of an Ikeda-like oscillator [6], [7]. In their simplest architecture, these oscillators are generally characterized by a continuous-wave (CW) laser seeding a Mach-Zehnder (MZ) electro-optical oscillator. The modulated signal travels through a long fiber delay line and, subsequently, is photodetected. The transduced electric signal is then filtered, eventually amplified, and connected back to the MZ modulator. When the overall normalized gain is higher than unity, the

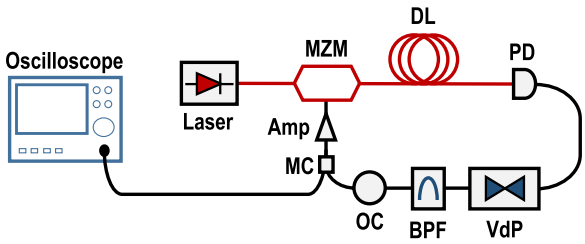

Fig. 1. Experimental setup for the multinonlinear electrooptic oscillator. MZM: Mach–Zehnder modulator; DL: delay line; PD: photodiode; VdP: Van der Pol circuit; BPF: bandpass filter (note that this element stands here for all the bandpass filtering elements of the electric branch); OC: offset controller; MC: microwave coupler; Amp: amplifier.

system oscillates via a Hopf bifurcation and simultaneously generates a microwave and a lightwave signal. The oscillator therefore features a continuous transduction of energy from the microwave to the lightwave frequency ranges, and *vice-versa.*

Two sub-families can be outlined, depending on the bandwidth of the electric branch in the feedback loop. On the one hand, when the filter is narrow, the dimensionality of the system is reduced and can be used to generate ultra-stable microwave signals [8]–[12]. Applications in this case are essentially in the area of aerospace engineering [13], sensing [14], and time-frequency metrology [15]–[19]. It should be emphasized that the coherent nature of the mutual coupling between the microwave and lightwave signals is one of the most important characteristics of this microwave photonic system, which can be used as well for pulse generation in optical fiber networks [20]–[24]. On the other hand, when the filter is broad, the oscillator has a very high dimensionality and can output hyperchaotic microwave signals [25]–[29]. Such broadband signals find their main applications when they are synchronized [30]–[34] for optical chaos communications [35] or when used for neuromorphic computing [36], [37].

The many applications related to this oscillator are a natural incentive to explore new architectures for this oscillator. In particular, it is noteworthy that the only nonlinearity of the system is the sinusoidal transfer function of the MZM. In fact, the electric branch of the feedback loop is always linear in the cases described above. However, implementing a nonlinear electronic feedback instead of a linear one permits to increase significantly the complexity of the oscillator and allow for new functionalities. In this paper, we explore a new architecture where the electronic branch of the feedback loop is nonlinear. We insert a self-sustained oscillator in the loop and investigate the various dynamical states generated when the system is in the oscillatory regime.

The article is organized as follows. In Section 2, we describe and characterize the nonlinearity of the electric branch in the feedback loop. Section 3 is devoted to the description of the full multi-nonlinear electro-optic oscillator. The complex dynamics of the system is studied in Section 4, where we analyze the breather and pulse-package dynamics of the system in the temporal domain and in the state-space. The last section will conclude this paper.

2. The System

In this section, we describe the architecture of the electro-optic oscillator with delayed feedback. The schematic representation of this system is presented in Fig. 1. The optical signal in the feedback loop is provided by a continuous-wave Distributed Bragg Reflector (DBR) semiconductor laser. It delivers up to 12 mW with a pump current of 100 mA, at the telecom wavelength $\lambda = 1559.8$ nm. The threshold of this laser is obtained for a pump current measured at $I_{\text{th}} = 27.3$ mA. The laser seeds an electro-optic lithium niobate Mach-Zehnder modulator (MZM), characterized by a RF half-wave voltage $V_{\pi\text{RF}}$ and DC voltage $V_{\pi\text{DC}}$. The transfer function of the MZ modulator is characterized by a sinusoidal nonlinearity, which allows for the control of the output optical power using voltages applied at the RF and DC electrodes of the modulator. The output signal of the MZM travels through an optical fiber of length $L = 100$ m, which

induces a time delay $T = n_g L/c = 0.5\ \mu$s, where $n_g = 1.5$ is the group velocity index of the fiber at telecom wavelength, and c is the velocity of light in vacuum. The delayed optical signal is detected by a fast photodiode with an optical/electrical conversion factor $S = 0.95$ A/W. This electric signal is fed to a Van der Pol circuit whose output is offset-controlled, amplified, and fed back to the DC electrode of the MZM. The overall bandwidth of the feedback loop is mainly controlled by the buffer amplifier in the electric branch and is experimentally found to span from $f_L = 13$ Hz (low cut-off frequency) to $f_H = 2.66$ MHz (high cut-off frequency).

The dynamical property of the system are usually ruled by the spectral properties of the bandpass filter and by the nonlinearity of the MZ transfer function [38]–[40]. In the present case, the nonlinearity of the Van der Pol oscillator will play an essential role as well.

3. The Nonlinear Feedback Loop

As indicated above, the two nonlinear interactions in the feedback loop occur in the MZM and in the Van der Pol circuit.

The nonlinear transfer function of the MZ modulator can be explicitly expressed as $P_{\text{out}} = P\cos^2[\pi u(t)/2V_\pi + \pi V_B/2V_\pi]$, where P is the power of the laser, V_B is a bias voltage, and V_π is the half-wave voltage of the electrode where the signal $u(t)$ is coupled.

On the other hand, the Van der Pol circuit inserted in the electric branch of the feedback loop is a self-sustained oscillator consisting of a LC oscillator (of eigenfrequency $\omega_0 = 1/\sqrt{LC}$) with nonlinear negative damping. This nonlinear damping is experimentally implemented using diodes with current-voltage characteristic $i = I_0\ [\exp(u/u_{\text{th}}) - 1]$, where I_0 is the almost constant current in reverse direction and u_{th} is the threshold voltage of the diode. The diode can be used as a switch, and between the negative and positive voltages, we have a transition area for the diode resistance, which can be exploited to obtain the nonlinear (cubic) transfer function for the voltage. In order to obtain a symmetrical transfer function, we use four parallel tumble diodes with a variable resistor, so that the dimensionless voltage $x(t)$ of the Van der Pol circuit obeys the well-known equation $\ddot{x} + \omega_0^2 x - \varepsilon(1 - x^2)\dot{x} = 0$, where ε is the nonlinear gain of the oscillator. Our Van der Por circuit can be tuned to output stable limit-cycles with frequencies ranging from 2 to 8 kHz. It should be noted that for being an autonomous two-dimensional dynamical system, the Van der Pol circuit cannot display chaos (Poincaré-Bendixon theorem). From the experimental standpoint, the strong feedback and non-ideality of the components of the circuit might lead to poor stability margins. Consequently, the system may be unstable when connected to strongly capacitive loads. In this case, a lag compensation network (for example, connecting the load to the voltage follower through a resistor) can be used to restore stability. A voltage follower is connected in the output of the nonlinear resistance and another one is connected in the output of inductor which is the principal output of Van der Pol oscillator. For impedance matching purposes, we using a buffer amplifier associated to an offset controlled. These elements are useful to define the offset of the MZ and to eliminate the loading effects.

The model of the system depends on two variables u_1 and u_2 which are the voltages at the output of the Van der Pol circuit and of the bandpass filter. The main parameters of the system are the gain of the loop, the offset phase of the MZM, and the time constants τ and θ standing for the cut-off times of the cascaded low- and high-pass filters, respectively. It should be noted that even though linear, our band-pass filter cannot be rigorously considered as a cascade of first order low-pass and high-pass filters modeled by an typical integro-differential operator as in refs. [25], [26]. Instead, realistic modeling would require to consider a linear filter operator $\hat{\mathcal{F}}$ featuring higher order integro-differential terms.

4. Breather and Pulse-Package Dynamics

The principal tunable parameter of the electro-optic oscillator is the laser power P, which is controlled by the pump current I. The operating point $\phi = \pi V_B/2V_\pi$ of the MZM has been set to $\pi/4$ throughout the paper.

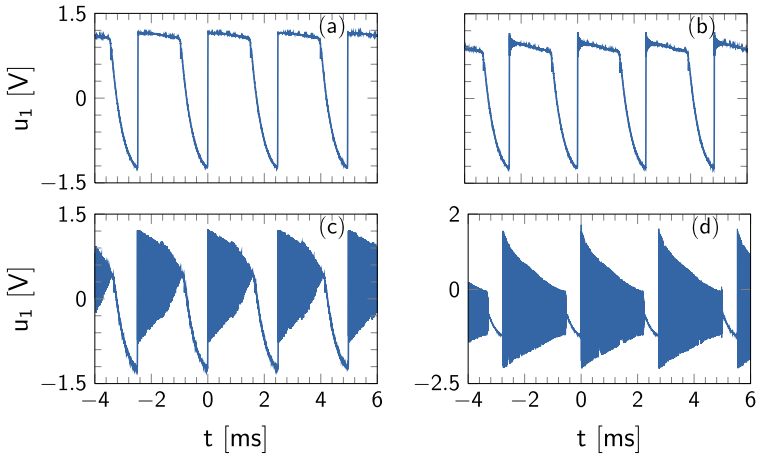

Fig. 2. Birth and evolution of breathers in the time domain as the laser pump current is increased beyond threshold ($T = 0$). (a) $I \simeq I_{th} = 27.3$ mA. (b) $I = 1.23\ I_{th}$. (c) $I = 1.49\ I_{th}$. (d) $I = 1.72\ I_{th}$.

In order to explore experimentally the complex dynamics of the oscillator, we first consider the case where the time delay is set to zero (the delay line is removed). When the laser current is increased beyond threshold, we first observe an hybrid regime where the oscillations are (multi-)periodic, as displayed in Fig. 2(a)–(d). For example, it can be seen in Fig. 2(a) that just above threshold, the output voltage of the oscillator is a single-frequency limit-cycle with frequency $f = 0.91$ kHz, which is of the same order of magnitude as the oscillation frequency for the uncoupled Van der Pol circuit. As the pump current I (and correspondingly, the laser power P) is increased, quasi-square-wave oscillations emerge at the sharp rising edge of the relaxation oscillations [see Fig. 2(b)], but they are rapidly damped shortly after their birth. At this stage, these emerging breathers are still periodic: the frequency of the slow oscillations is 0.83 kHz while the frequency of the fast (damped) oscillations is 258 kHz. As the laser power is increased, we observe a fast-scale dynamics is superimposed onto a slow-scale limit cycle, as displayed in Fig. 2(c) and (d). For these periodic breathers, the frequencies of the fast oscillations are equal to 72 kHz and 430 kHz respectively, while the slow oscillation frequency remains almost the same, on the order of 1 kHz.

Still, with null delay, we find that further increase of the pump current drives the system in a regime of complex oscillations involving chaotic breathers and pulse-package oscillations. In Fig. 3(a), we observed the first chaotic breathers, characterized by a chaotic fast-scale oscillation superimposed onto a periodic slow-scale oscillation. Then, higher pump power leads to a dynamical state corresponding to chaotic pulse-package oscillations [see Fig. 3(b)]. Further increase of the pump power leads to a reverse bifurcation where the system becomes bi-periodic, and then periodic in time [see Fig. 3(c) and (d)]. Better understanding of the timetraces displayed in Fig. 3 can be achieved using the phase portrait plots of Fig. 4. For example, Fig. 4(a) shows the inherent slow-fast structure of the chaotic attractor, which has strongly repelling eigendirection around which the trajectory is twisted. On the other hand, the chaotic attractor of the pulse-packages displayed in Fig. 4(b) features an asymmetric double-scroll structure. This dynamical pattern is singular in several aspects and has never been reported experimentally to the best of our knowledge. Fig. 4(c) and (d) evidences the periodic nature of the temporal output signal from Fig. 3(c) and (d).

When the time-delay is accounted for (insertion of the optical fiber of length 100 m), the system becomes infinite-dimensional, and it has the potential to feature other complex behaviors. In Fig. 5(a) and (b), it can be seen that when the laser is pumped just above threshold, we obtain relaxation oscillations and breathers comparable to those obtained with null delay [see Fig. 2(a) and (b)]. However, when we increase the pump power, the system outputs

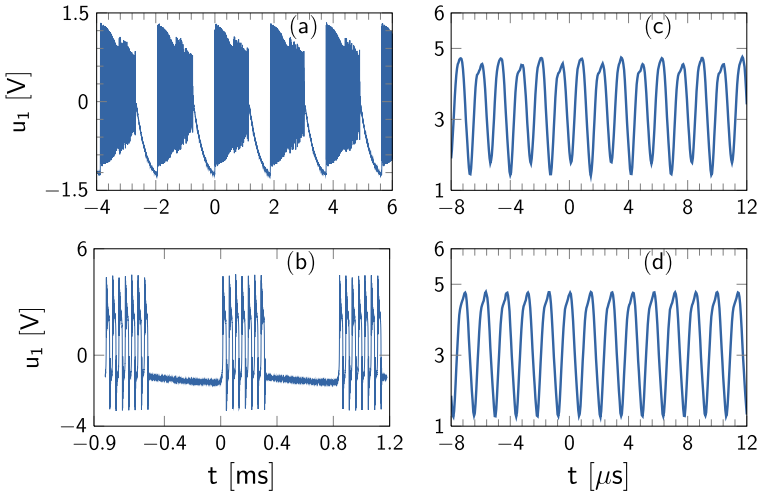

Fig. 3. Evolution and death of the breathers and pulse-package oscillations in the time domain as the laser pump current is increased far above threshold ($T = 0$). (a) $I = 1.81\ I_{th}$. (b) $I = 2.27\ I_{th}$. (c) $I = 2.77\ I_{th}$. (d) $I = 2.93\ I_{th}$.

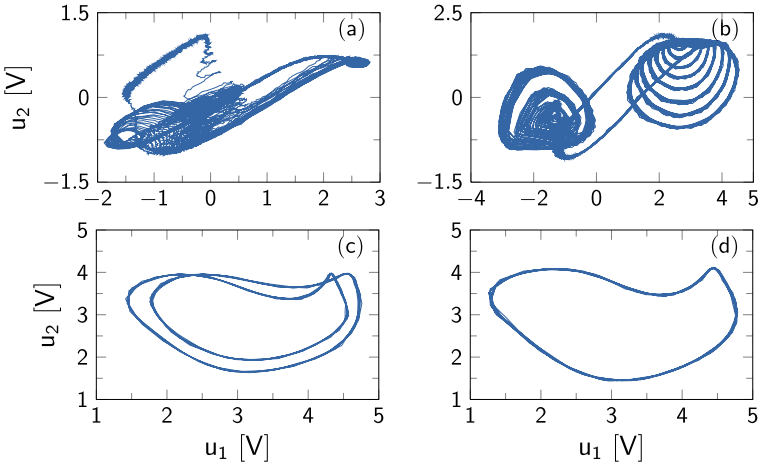

Fig. 4. Evolution and death of the breathers and pulse-package oscillations in the phase space as the laser pump current is increased far above threshold ($T = 0$). These figures correspond to the time traces displayed in Fig. 3. (a) $I = 1.81\ I_{th}$. (b) $I = 2.27\ I_{th}$. (c) $I = 2.77\ I_{th}$. (d) $I = 2.93\ I_{th}$.

pulse-package oscillations that are chaotic [see Fig. 5(c)], while those obtained when $T = 0$ are periodic. Further increase of the laser power leads to fully developed hyperchaos, as displayed in Fig. 2(d). In this latter case, the underlying structure of the pulse-packages is totally lost.

The enlargements displayed in Fig. 6(a) and (b) display the inner structure of the pulse-package oscillations of Figs. 2(b) and 3(c), which evidence the second and third (fastest) timescales. The first timescale (not displayed) is the slowest oscillation and has a typical frequency of the order of 1 kHz, which corresponds to the range the frequency of the Van der Pol self-sustained oscillations. The second timescale rules the frequency if the pulse-packages and is typically of the order of 20 kHz. The third and fastest timescale has a typical frequency of the order of 800 kHz. The main difference between the cases with and without delay is the nature of the fastest oscillation, which is periodic in the first case but chaotic in the second. A multi-loop

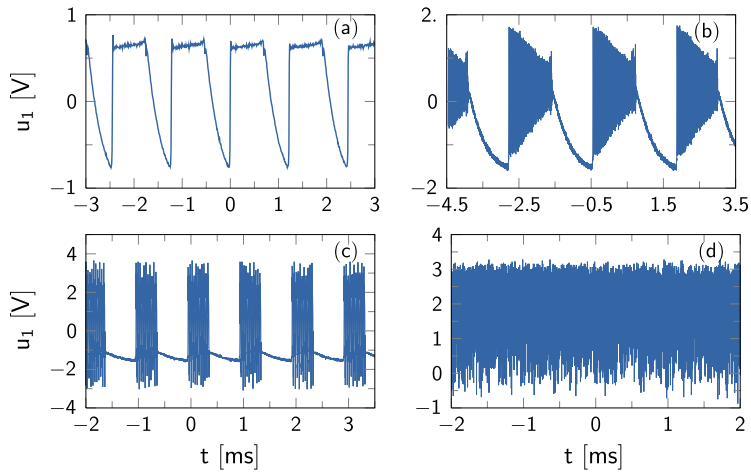

Fig. 5. Breathers, pulse-package oscillations, and fully developed hyperchaos as the laser pump current is increased far above threshold in the presence of delay ($T = 0.5\ \mu$s). (a) $I = 1.28\ I_{th}$. (b) $I = 1.64\ I_{th}$. (c) $I = 2.46\ I_{th}$. (d) $I = 3.34\ I_{th}$.

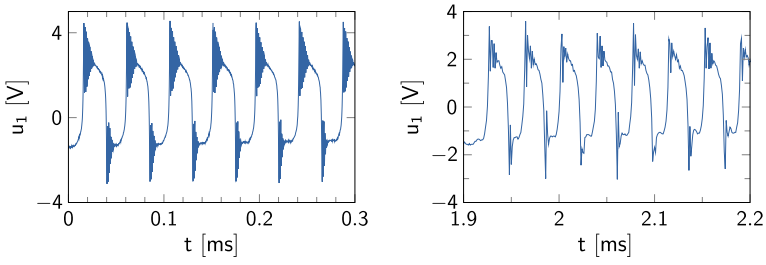

Fig. 6. Evidence of the three-timescale behavior of the system in the pulse-package regime. (Left) Enlargement of pulse packages for the system without delay and with $I = 2.27\ I_{th}$ [see Fig. 3(b)]. The fastest oscillations are periodic. (Right) Enlargement of pulse packages with delay and with $I = 2.46\ I_{th}$ [see Fig. 5(c)]. The fastest oscillations are chaotic.

architecture (see, for example, [41]–[44]) would provide extra-degrees of freedom and therefore, a wider variety of dynamical behaviors whenever a nonlinear element is inserted into the feedback loop.

5. Conclusion

In this paper, we have analyzed experimentally the complex dynamical behavior of a multi-nonlinear electro-optical system with feedback. We have evidenced breather and pulse-package oscillations in the system, in both the periodic and chaotic regimes. These states are characterized by a slow-fast temporal dynamics originating from two or three split timescales.

This study has shown that coupling a nonlinear self-sustained circuit to a photonic oscillator provides a wide range of new dynamical behaviors which open the door for new applications. For example, neuromorphic computing using electro-optical systems with feedback could benefit from the pulse-package capability which is reminiscent of the firing behavior of neurons. Self-sustained oscillator could also provide a tool to achieve (sub-)harmonic phase-locking for a certain class of microwave photonics oscillators. Further research will be devoted to the exploration of these potential applications, in particular when several such oscillators are coupled for synchronization purposes [45]–[47].

Acknowledgment

The authors would also like to acknowledge fruitful interactions with L. Larger for the design of the nonlinear feedback loop.

References

[1] T. Erneux, *Applied Delay Differential Equations*. New York, NY, USA: Springer-Verlag, 2010.
[2] M. Lakshamanan and D. V. Senthikumar, *Dynamics of Nonlinear Time-Delay Systems*. Berlin, Germany: Springer-Verlag, 2011.
[3] L. Larger, "Complexity in electro-optic delay dynamics: Modelling, design and applications," *Phil. Trans. R. Soc. A*, vol. 371, 2013, Art. no. 20120464.
[4] M. C. Soriano, J. Garcia-Ojalvo, C. R. Mirasso, and I. Fischer, "Complex photonics: Dynamics and applications of delay-coupled semiconductors lasers," *Rev. Mod. Phys.*, vol. 85, pp. 421–470, 2013.
[5] A. Neyer and E. Voges, "Dynamics of electrooptic bistable devices with delayed feedback," *IEEE J. Quantum Electron.*, vol. QE-18, no. 12, pp. 2009–2015, Dec. 1982.
[6] K. Ikeda, "Multiple-valued stationary state and its instability of the transmitted light by a ring cavity system," *Opt. Commun.*, vol. 30, pp. 257–261, 1979.
[7] K. Ikeda, H. Daido, and O. Akimoto, "Optical turbulence: Chaotic behavior of transmitted light from a ring cavity," *Phys. Rev. Lett.*, vol. 45, pp. 709–712, 1980.
[8] X. S. Yao and L. Maleki, "High frequency optical subcarrier generator," *Elect. Lett.*, vol. 30, pp. 1525–1526, 1994.
[9] X. S. Yao and L. Maleki, "Optoelectronic microwave oscillator," *J. Opt. Soc. Amer. B, Opt. Phys.*, vol. 13, pp. 1725–1735, 1996.
[10] Y. K. Chembo, L. Larger, H. Tavernier, R. Bendoula, E. Rubiola, and P. Colet, "Dynamic instabilities generated with optoelectronic oscillators," *Opt. Lett.*, vol. 32, pp. 2571–2573, 2007.
[11] Y. K. Chembo, L. Larger, R. Bendoula, and P. Colet, "Effects of gain and bandwidth on the multimode behavior of optoelectronic microwave oscillators," *Opt. Exp.*, vol. 16, pp. 9067–9072, 2008.
[12] Y. K. Chembo, L. Larger, and P. Colet, "Nonlinear dynamics and spectral stability of optoelectronic microwave oscillators," *IEEE J. Quantum Electron.*, vol. 44, no. 9, pp. 858–866, Sep. 2008.
[13] L. Maleki, "The optoelectronic oscillator," *Nature Photon.*, vol. 5, pp. 728–730, 2011.
[14] X. Zou *et al.*, "OptoElectronic Oscillators (OEOs) to sensing, measurement, and detection," *IEEE J. Quantum Electron.*, vol. 52, no. 1, 2016, Art. no. 0601116.
[15] S. Romisch, J. Kitching, E. Ferre-Pikal, L. Hollberg, and F. L. Walls, "Performance evaluation of an optoelectronic oscillator," *IEEE Trans. Ultrason., Ferroelectr., Freq. Control*, vol. 47, no. 5, pp. 1159–1165, Sep. 2000.
[16] C. Williams, J. D. Rodriguez, D. Mandridis, and P. J. Delfyett, "Noise characterization of an injection-locked COEO with long-term stabilization," *J. Lightw. Technol.*, vol. 29, pp. 2906–2912, 2011.
[17] O. Okusaga *et al.*, "Spurious mode reduction in dual injection-locked optoelectronic oscillators," *Opt. Exp.*, vol. 19, no. 7, pp. 5839–5854, 2011.
[18] Y. Zhang, D. Hou, and J. Zhao, "Long-term frequency stabilization of an optoelectronic oscillator using phase-locked loop," *IEEE J. Lightw. Technol.*, vol. 32, no. 13, pp. 2408–2414, Jul. 2014.
[19] K. Saleh, G. Lin, and Y. K. Chembo, "Effect of laser coupling and active stabilization on the phase noise performance of optoelectronic microwave oscillators based on whispering-gallery-mode resonators," *IEEE Photon. J.*, vol. 7, no. 1, Feb. 2014, Art. no. 5500111.
[20] X. S. Yao, L. Davis, and L. Maleki, "Coupled optoelectronic oscillators for generating both RF signal and optical pulses," *IEEE J. Lightw. Technol.*, vol. 18, no. 1, pp. 73–78, Jan. 2000.
[21] J. Lasri *et al.*, "A self-starting hybrid optoelectronic oscillator generating ultra low jitter 10-GHz optical pulses and low phase noise electrical signals," *IEEE Photon. Technol. Lett.*, vol. 14, no. 7, pp. 1004–1006, Jul. 2002.
[22] Y. K. Chembo, A. Hmima, P.-A. Lacourt, L. Larger, and J. M. Dudley, "Generation of ultralow jitter optical pulses using optoelectronic oscillators with time-lens soliton-assisted compression," *IEEE J. Lightw. Technol.*, vol. 27, no. 22, pp. 5160–5167, Nov. 2009.
[23] N. Huang, M. Li, Y. Deng, and N. H. Zhu, "Optical pulse generation based on an optoelectronic oscillator with cascaded nonlinear semiconductor optical amplifiers," *IEEE Photon. J.*, vol. 6, no. 1, 2014, Art. no. 5500208.
[24] S. Jia *et al.*, "A novel highly stable dual-wavelength short optical pulse source based on a dual-loop optoelectronic oscillator with two wavelengths," *IEEE Photon. J.*, vol. 7, no. 4, Aug. 2015, Art. no. 1502611.
[25] J.-P. Goedgebuer, P. Levy, L. Larger, C.-C. Chen, and W. T. Rhodes, "Optical communication with synchronized hyperchaos generated electrooptically," *IEEE J. Quantum Electron.*, vol. 38, no. 9, pp. 1178–1183, Sep. 2002.
[26] Y. C. Kouomou, P. Colet, L. Larger, and N. Gastaud, "Chaotic breathers in delayed electro-optical systems," *Phys. Rev. Lett.*, vol. 95, 2005, Art. no. 203903.
[27] K. E. Callan, L. Illing, Z. Gao, D. J. Gauthier, and E. Scholl, "Broadband chaos generated by an optoelectronic oscillator," *Phys. Rev. Lett.*, vol. 104, 2010, Art. no. 113901.
[28] L. Weicker *et al.*, "Strongly asymmetric square waves in a time-delayed system," *Phys. Rev. E, Stat. Phys. Plasmas Fluids Relat. Interdiscip. Top.*, vol. 86, 2012, Art. no. 055201.
[29] L. Weicker *et al.*, "Slow-fast dynamics of a time-delayed electro-optic oscillator," *Phil. Trans. R. Soc. A*, vol. 371, 2013, Art. no. 20120459.
[30] A. B. Cohen, B. Ravoori, T. E. Murphy, and R. Roy, "Using synchronization for prediction of high-dimensional chaotic dynamics," *Phys. Rev. Lett.*, vol. 101, 2008, Art. no. 154102.
[31] T. E. Murphy *et al.*, "Complex dynamics and synchronization of delayed-feedback nonlinear oscillators," *Phil. Trans. R. Soc. A*, vol. 368, pp. 343–366, 2010.

[32] B. Ravoori, A. B. Cohen, J. Sun, A. E. Motter, T. E. Murphy, and R. Roy, "Robustness of optimal synchronization in real networks," *Phys. Rev. Lett.*, vol. 107, 2011, Art. no. 034102.
[33] L. Illing, G. Hoth, L. Shareshian, and C. May, "Scaling behavior of oscillations arising in delay-coupled optoelectronic oscillators," *Phys. Rev. E, Stat. Phys. Plasmas Fluids Relat. Interdiscip. Top.*, vol. 83, 2011, Art. no. 026107.
[34] L. Illing, C. D. Panda, and L. Shareshian, "Isochronal chaos synchronization of delay-coupled optoelectronic oscillators," *Phys. Rev. E, Stat. Phys. Plasmas Fluids Relat. Interdiscip. Top.*, vol. 84, 2011, Art. no. 016213.
[35] A. Argyris *et al.*, "Chaos-based communications at high bit rates using commercial fibre-optic links," *Nature*, vol. 438, no. 7066, pp. 343–346, Nov. 2005.
[36] L. Larger *et al.*, "Photonic information processing beyond Turing: An optoelectronic implementation of reservoir computing," *Opt. Exp.*, vol. 20, pp. 3241–3249, 2012.
[37] R. Martinenghi, S. Rybalko, M. Jacquot, Y. K. Chembo, and L. Larger, "Photonic nonlinear transient computing with multiple-delay wavelength dynamics," *Phys. Rev. Lett.*, vol. 108, 2012, Art. no. 244101.
[38] A. F. Talla *et al.*, "Analysis of phase-locking in narrow-band optoelectronic oscillators with intermediate frequency," *IEEE J. Quantum Electron.*, vol. 51, no. 6, Jun. 2015, Art. no. 5000108.
[39] J. H. T. Mbé *et al.*, "Mixed-mode oscillations in slow-fast delayed optoelectronic systems," *Phys. Rev. E, Stat. Phys. Plasmas Fluids Relat. Interdiscip. Top.*, vol. 91, no. 1, 2015, Art. no. 12902.
[40] G. R. G. Chengui *et al.*, "Theoretical and experimental study of slow-scale Hopf limit-cycles in laser-based wideband optoelectronic oscillators," *J. Opt. Soc. Amer. B, Opt. Phys.*, vol. 31, no. 10, pp. 2310–2316, 2014.
[41] E. Shumakher and G. Eisenstein, "A novel multiloop optoelectronic oscillator," *IEEE Photon. Technol. Lett.*, vol. 22, no. 22, pp. 1881–1883, Nov. 2008.
[42] E. C. Levy *et al.*, "Comprehensive computational model of single-and dual-loop optoelectronic oscillators with experimental verification," *Opt. Exp.*, vol. 18, pp. 21461–21476, 2010.
[43] R. M. Nguimdo, Y. K. Chembo, P. Colet, and L. Larger, "On the phase noise performance of nonlinear double-loop optoelectronic microwave oscillators," *IEEE J. Quantum Electron.*, vol. 48, no. 11, pp. 1415–1423, Nov. 2012.
[44] X. Liu, W. Pan, X. Zou, B. Luo, L. Yan, and B. Lu, "A reconfigurable optoelectronic oscillator based on cascaded coherence-controllable recirculating delay lines," *Opt. Exp.*, vol. 20, pp. 13296–13301, 2012.
[45] Y. C. Kouomou and P. Woafo, "Generalized correlated states in a ring of coupled nonlinear oscillators with a local injection," *Phys. Rev. E, Stat. Phys. Plasmas Fluids Relat. Interdiscip. Top.*, vol. 66, 2002, Art. no. 066201.
[46] Y. C. Kouomou and P. Woafo, "Transitions from spatiotemporal chaos to cluster and complete synchronization states in a shift-invariant set of coupled nonlinear oscillators," *Phys. Rev. E, Stat. Phys. Plasmas Fluids Relat. Interdiscip. Top.*, vol. 67, no. 4, 2003, Art. no. 046205.
[47] Y. C. Kouomou and P. Woafo, "Cluster synchronization in coupled chaotic semiconductor lasers and application to switching in chaos-secured communication networks," *Opt. Commun.*, vol. 223, pp. 283–293, 2003.